VOLUME 11 ISSUE 2 2025

ISSN 2454 – 3055

INTERNATIONAL JOURNAL OF ZOOLOGICAL INVESTIGATIONS

Forum for Biological and Environmental Sciences

Published by Saran Publications, India

International Journal of Zoological Investigations Vol. 11, No. 2, 1106-1116 (2025)

International Journal of Zoological Investigations
Contents available at Journals Home Page: www.ijzi.net
Editor-in-Chief: Prof. Ajai Kumar Srivastav
Published by: Saran Publications, Gorakhpur, India

ISSN: 2454-3055

Green Synthesis of Silver Doped Zinc Oxide Nanoparticles using Madras Carpet (*Grangea maderaspatana*) and its Antibacterial Activity against *Pseudomonas aeruginosa* and *Listeria monocytogenes*

Shukla Yogesh Kumar[1], Pandey Priyansh[1], Srivastava Ashok Kumar[2], Singh Saurabh Pratap[1], Pandey Janardan Prasad[1], Kumar Jitendra[3] and Shukla Alok[1]*

[1]Department of Physics, M.L.K. P.G. College, Balrampur 271201, Uttar Pradesh, India
[2]Department of Physics, SRM Institute of Science and Technology, Chennai 6000, Tamil Nadu, India
[3]Department of Chemistry, M.L.K. P.G. College, Balrampur 271201, Uttar Pradesh, India

**Corresponding Author*

Received: 26th October, 2025; **Accepted:** 10th December, 2025; **Published online:** 15th December, 2025

https://doi.org/10.33745/ijzi.2025.v11i02.111

Abstract: Present study entails the green synthesis of silver doped ZnO nanoparticles (Ag-ZnO) using aqueous plant extract of *Grangea maderaspatana* also commonly known as Madras Carpet. Various techniques such as UV-visible, PXRD, FTIR, SEM, and EDS were used for characterization of final synthesized materials and to confirm the synthesis of Ag-ZnO. PXRD spectrum suggested high crystallinity of the material and the average crystallite size as per Debye Sherer's formula was 14.52 nm. SEM images revealed the spherical shape of particles and average size of 49.4 nm. UV-visible spectroscopy revealed the characteristic peak at 379 nm and band gap of 2.21 eV. Additionally, antibacterial efficacy of the material was tested against two bacterial strains *Listeria monocytogenes* and *Pseudomonas aeruginosa*, at the dose concentrations of 100 µg/ml, 200 µg/ml and 300 µg/ml. Significant zone of inhibition was observed against both strains, confirming its antibacterial efficacy.

Keywords: Nanocomposite, Bimetallic, *Grangea maderaspatana*, *Listeria monocytogenes*, *Pseudomonas aeruginosa*, Green synthesis, Antibacterial

Citation: Shukla Yogesh Kumar, Pandey Priyansh, Srivastava Ashok Kumar, Singh Saurabh Pratap, Pandey Janardan Prasad, Kumar Jitendra and Shukla Alok: Green synthesis of silver doped zinc oxide nanoparticles using Madras Carpet (*Grangea maderaspatana*) and its antibacterial activity against *Pseudomonas aeruginosa* and *Listeria monocytogenes.* Intern. J. Zool. Invest. 11(2): 1106-1116, 2025.

https://doi.org/10.33745/ijzi.2025.v11i02.111

Introduction

Nanotechnology has offered materials with unique optical, electronic, and biological properties to combat global challenges (Kirubakaran *et al.*, 2025). With the rapid advancement of nanotechnology, metal/semiconductor nano-composites, consisting of one metal and other metal oxide, exhibit synergistic effects that surpass the antimicrobial activities of their monometallic counterparts, offering a broad spectrum of physiochemical properties and diverse mechanisms of action.

One of the most explored semiconductor nanoparticles (NPs), ZnONPs are a good choice for many medicinal applications because of their effective anti-bacterial activity against a variety of harmful bacteria (Aldeen *et al.*, 2022). One of the reason to choose this lies in the fact that it is generally recognized as safe (GRAS) by the FDA (21 CFR 182.8991)(Shukla *et al.*, 2025). Numerous attempts have been made to create nano-composite structures by doping ZnO with noble metals(Pd, Ag, Pt, Au)(Liu *et al.*, 2017). Since Ag is most cost effective among other noble metals and inherently antimicrobial (Baig *et al.*, 2025), it is often chosen as dopant in metal/ZnO nano-composites (Liu *et al.*, 2017). Depending on their intended function, Ag doped ZnO NPs are prepared using a variety of chemical and physical processes to produce a range of sizes and forms. The most popular techniques are sputtering, chemical vapour deposition, microwave-assisted thermal evaporation, sol-gel, infrared irradiation, pulsed laser deposition, and electrochemical reactions (Jose' Luis *et al*, 2022; Triphati and Pirzadah, 2023). Most of these methods are energy intensive and often turn out to be costly (Bahramikia and Izadi, 2023).

In recent years, there has been growing academic attention toward biosynthetic approaches, commonly referred to as green synthesis (Bahramikia and Izadi, 2023). Compared to traditional physical and chemical methods, this strategy offers multiple advantages such as operational simplicity, cost-effectiveness, environmental compatibility, scalability, and the absence of hazardous reagents, resulting in more stable and biocompatible nanoparticles (Kandav and Sharma, 2024). Among the diverse biosynthetic routes reported encompassing bacteria, fungi, and enzyme-mediated systems-- plant extract-based green synthesis has emerged as the most promising and sustainable alternative for nanoparticle production (El-Seedi *et al.*, 2024). In many previous reports, Silver doped ZnO nanoparticles were synthesized using different plant extracts such as *Azadirachta indica* leaves (Iqbal *et al.*, 2021), *Ruta chalepensis* leaves (Hunde Gonfa and Lealem Birhanu, 2024), *Moringa oleifera* extract (Verma *et al.*, 2020), and *Vitis vinifera* leaves (Saravanadevi *et al.*, 2022) for the antibacterial activity.

In this context, the aqueous extract from Madras carpet (*Grangea maderaspatana* (L.)) has been employed for the synthesis of Ag-ZnO NPs. Abundant phytochemical constituents and medicinal value of *Grangea maderaspatana* (L.) were key motivation choosing this plant (Thanuja *et al.*, 2024). Phytochemical investigations of *G. maderaspatana* have revealed the presence of several active compounds, including flavonoids, terpenoids, steroids, tannins, saponins, and phenolics. These metabolites play dual roles as reducing and stabilizing agents preventing agglomeration and enhancing surface reactivity. *G. maderaspatana* is also renowned for its analgesic, anti-inflammatory, antipyretic diuretic, antioxidant, antidiabetic and gastro-protective properties and is traditionally employed in Ayurvedic medicine to alleviate ailments such as rheumatism, gastrointestinal disturbances, and microbial infections (Thanuja *et al.*, 2024; Deepa Rani *et al.*, 2025). In the present study, for establishing the antibacterial efficacy of synthesized Ag doped ZnO, it was tested against two microbial strains *L. monocytogenes* and *P. aeruginosa.*

Materials and Methods

Materials

All the chemicals were purchased from standard chemical suppliers and been used without any additional purification. Zinc acetate dihydrate ($(CH_3.COO)_2$ $Zn.2H_2O$), 98.5%) (Product Code: Q28755 and CAS No. 5970-45-6) and Silver Nitrate ($AgNO_3$, 99.8 %) (Product code 27462 and CAS No. 7761-88-8) was used as host and dopant metal precursors. Distilled water was used throughout the experiment.

Plant collection and extract preparation

Madras carpet plant was collected from a dried pond floor close to the M.L.K. P.G. College campus. To ensure they were completely free from any impurity and other plant, these were periodically washed with running tap water and closely inspected before subjecting it to drying overnight at 50 °C in an oven. After that, the dried pants were ground into a fine powder using a home mixer. Following that, it was kept for later use in an airtight container. 20 g of this plant powder was added to 100 ml of distilled water and heated to 60°C while maintaining continuously to produce the extract for 1 h, while being constantly stirred. Afterwords, this concoction was filtered using 40 GSM Whatman Filter paper. The solution was also centrifuged at 5000 rpm to further sediment the bigger particles. The decanted extract solution was filtered again using filter paper and stored in a reagent bottle in the refrigerator.

Synthesis of Ag-ZnO

0.01 M $AgNO_3$ and 1 M Zinc acetate solution, 50 ml of each is dropwise added simultaneously in a flask containing 20 ml aqueous plant extract with continuous stirring. After 30 min temperature was turned on to facilitate the reaction and was maintained at 60 °C for 90 min. The synthesis was confirmed by the onset of visible precipitate formation. This precipitate was separated by subjecting this solution to centrifugation at 7000 rpm. Then collected material was thoroughly washed multiple times using distilled water to remove any impurity and placed in a hot air oven for drying. After complete drying, the material was crushed and ground to fine powder using mortar pestle. This powder was then stored in an airtight sample plastic sample container for characterization and analysis.

Characterization

Functional groups present on the nanoparticle surfaces were characterized using a Fourier Transform-Infrared Spectrometer (Model: Nicole 6700, Make: Thermo-Scientific, USA) equipped with an Attenuated Total Reflectance (ATR) accessory. The optical properties of the synthesized Cu NPs were analyzed using a Hitachi UH5300 double-beam spectrophotometer in the wavelength range of 300-800 nm. The surface morphology and elemental composition of the NPs were analyzed using a JEOL JSM 6490 Scanning Electron Microscope equipped with an OXFORD Instruments INCA x-act EDS detector. Crystallinity and phase identification of the synthesized NPs were determined using an X-ray diffractometer (Model: D8 Advance Eco, Make: Bruker, Germany).

Antibacterial Activity

The antibacterial activity of Ag/ZnO@MC was evaluated against two bacterial strains: *Pseudomonas aeruginosa* (*P. aeruginosa*) and *Listeria monocytogenes* (*L. monocytogenes*). These strains were consistently maintained and propagated on Mueller Hinton Agar (MHA). The antimicrobial activity of Ag/ZnO@MC was subsequently determined using the well diffusion method. For the preparation of the Mueller Hinton Agar (MHA) medium, 38 g of the MHA powder were precisely dissolved in 1 L of distilled water. This mixture was then subjected to sterilization by autoclaving at 121°C and 15 psi for 15 min. Following the sterilization process, the molten MHA was aseptically poured into sterile glass Petri dishes, with 25 ml dispensed per plate, under strictly controlled laminar airflow conditions, and subsequently allowed to solidify. Once the MHA plates had solidified, each plate was uniformly inoculated with a 24 h bacterial culture using a sterile cotton swab, ensuring the formation of an even bacterial lawn across the entire agar surface. Subsequent to inoculation, wells were precisely created in the inoculated agar using a sterile cork borer, each designed with an appropriate diameter to accommodate the test solutions. For the evaluation of antibacterial activity, 35 µl of Ag/ZnO@MC was carefully loaded into these wells. Ag/ZnO@MC was evaluated across three distinct concentrations: 100 µg/ml (designated as C1 well), 200 µg/ml (C2 well), and 300 µg/ml (C3 well). To ensure experimental validity, both

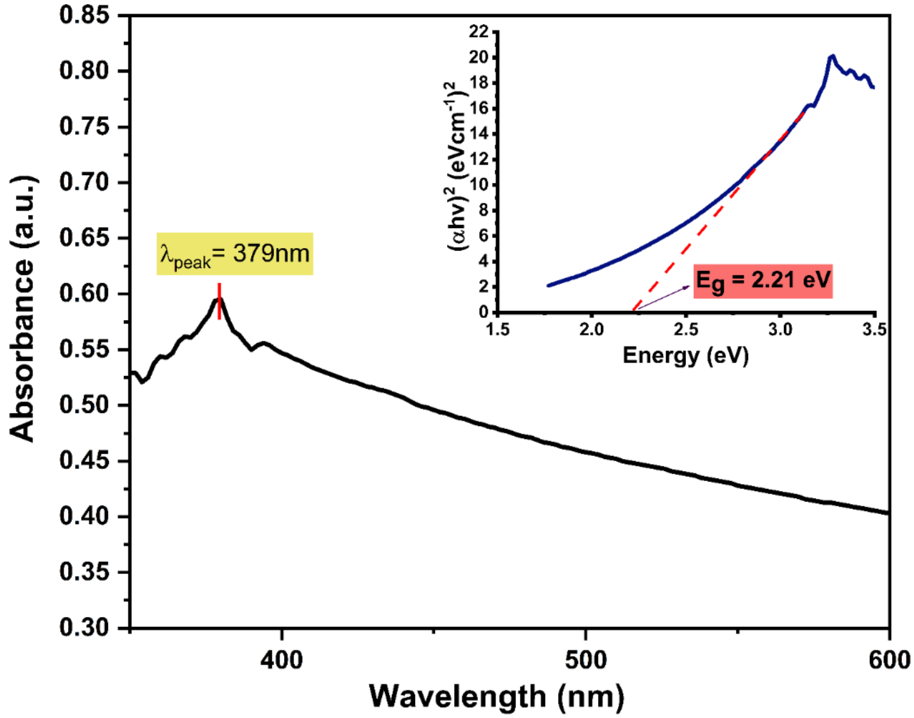

Fig. 1: UV Spectrum of Ag/ZnO@MC and Tauc Plot of the same (inset).

positive and negative controls were incorporated into each experiment. Ciprofloxacin (10 µl of a 200 ppm solution) served as the positive control, demonstrating expected inhibition, while 10 µl of sterile distilled water was utilized as the negative control to confirm the absence of inherent antimicrobial activity from the solvent. After the application of Ag/ZnO@MC and controls, the plates were meticulously sealed with paraffin to prevent any desiccation and then incubated at 37°C for a period of 24 h. Following this 24 h incubation, the plates were examined for the presence of clear zones around the wells. The diameter of these zones of inhibition was measured in millimeters (mm) using a ruler. Triplicate run for all assays were performed to ensure reproducibility.

Results and Discussion

UV-visible Analysis

The optical properties of the biosynthesized Ag/ZnO@MC material were investigated using UV-visible absorption spectroscopy (Fig. 1). The absorption spectrum exhibited a prominent peak at 379 nm, which corresponds to the intrinsic band-edge excitation of ZnO. This peak is consistent with previously reported values for ZnO nanoparticles and Ag-ZnO composites, which typically show absorption edges in the range of 375-380 nm.

To estimate the optical band gap energy (E_g), the Tauc plot method was employed, based on the relation:

$$(\alpha h\nu)^n = A(h\nu - E_g)$$

Where α is the absorption coefficient, $h\nu$ is the photon energy, A is a constant, E_g is the band gap energy, and n characterizes the nature of the electronic transition (here, $n = \frac{1}{2}$ for a direct allowed transition typical of ZnO). The Tauc plot was constructed by plotting $(\alpha h\nu)^2$ versus photon energy $(h\nu)$, and the extrapolation of the linear region to $(\alpha h\nu)^2 = 0$ yielded an estimated band gap of 2.21 eV (inset of Fig. 1).

The observed reduction in band gap relative to

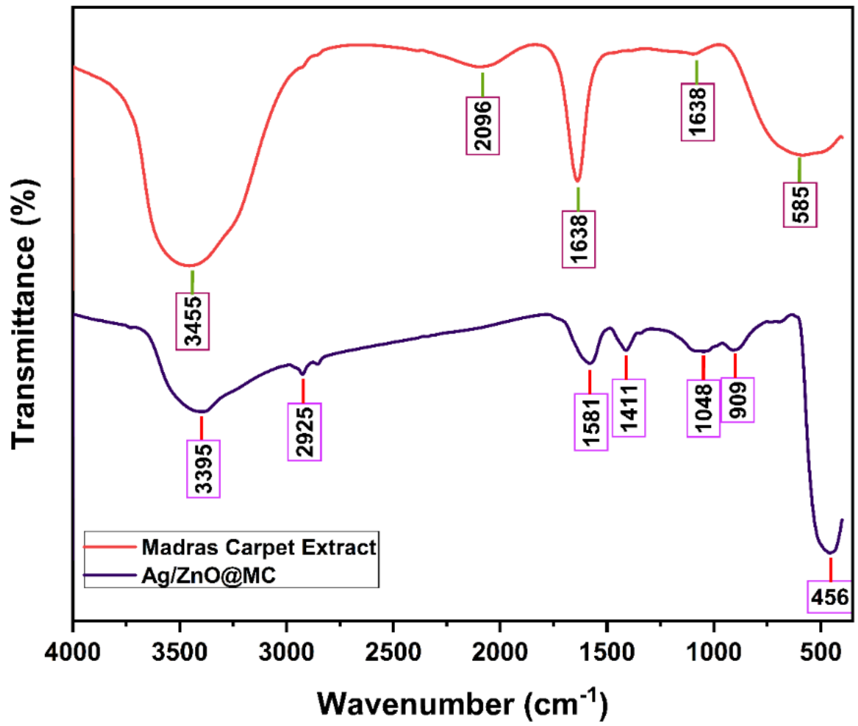

Fig. 2: FTIR spectrum of Ag/ZnO@MC.

bulk ZnO (~3.2 eV) is attributed to the incorporation of Ag nanoparticles in the lattice of ZnO.

FTIR

Fourier-transform infrared (FTIR) spectroscopy was conducted to probe the functional groups involved in the biosynthesis and stabilization of the Ag/ZnO nanocomposite mediated by *Grangea maderaspatana* (MC) plant extract. The spectra of the pure plant extract and the biosynthesized Ag/ZnO@MC composite were recorded with 32 scans each as shown in Figure 2.

Characteristic absorption bands from the plant extract were assigned to phytochemicals participating in the green synthesis, including a broad O–H stretching vibration around 3400 cm^{-1}, indicative of hydroxyl groups from phenolics and alcohols; C–H stretching vibrations near 2920 and 2850 cm^{-1} corresponding to aliphatic groups; and a strong C=O stretch near 1630 cm^{-1}, associated with carbonyl groups in flavonoids and other biomolecules (Pandey *et al.*, 2025). In the Ag/ZnO@MC nanocomposite spectrum, notable shifts and intensity changes of these peaks indicated involvement of hydroxyl and carbonyl groups in the capping and nanoparticle stabilization (Shreema *et al.*, 2021). The peaks at 1581 cm^{-1}, 1411 cm^{-1}, 1048 cm^{-1}, 909 cm^{-1} corresponds to the C=O asymmetric and symmetric stretching vibrations, C–O stretching, and C–H bending modes, respectively (Rathika and Irine, 2022). The Zn–O stretching vibrations are typically observed as strong absorption bands near 430–490 cm^{-1}. For example, peaks at around 466 cm^{-1} are commonly assigned to Zn–O bonds, confirming the formation of ZnO nanostructures (Atherton *et al.*, 1971; Pandey *et al.*, 2025).

SEM and EDS

As per SEM micrographs, the composite displayed a generally spherical-like and some random shapes which is common in green synthesized nanocomposites (Fig. 3a, b, d).

Individual particle diameters were measured using ImageJ, and these data points were used to generate a particle size distribution curve. The resulting histogram revealed that most Ag/ZnO

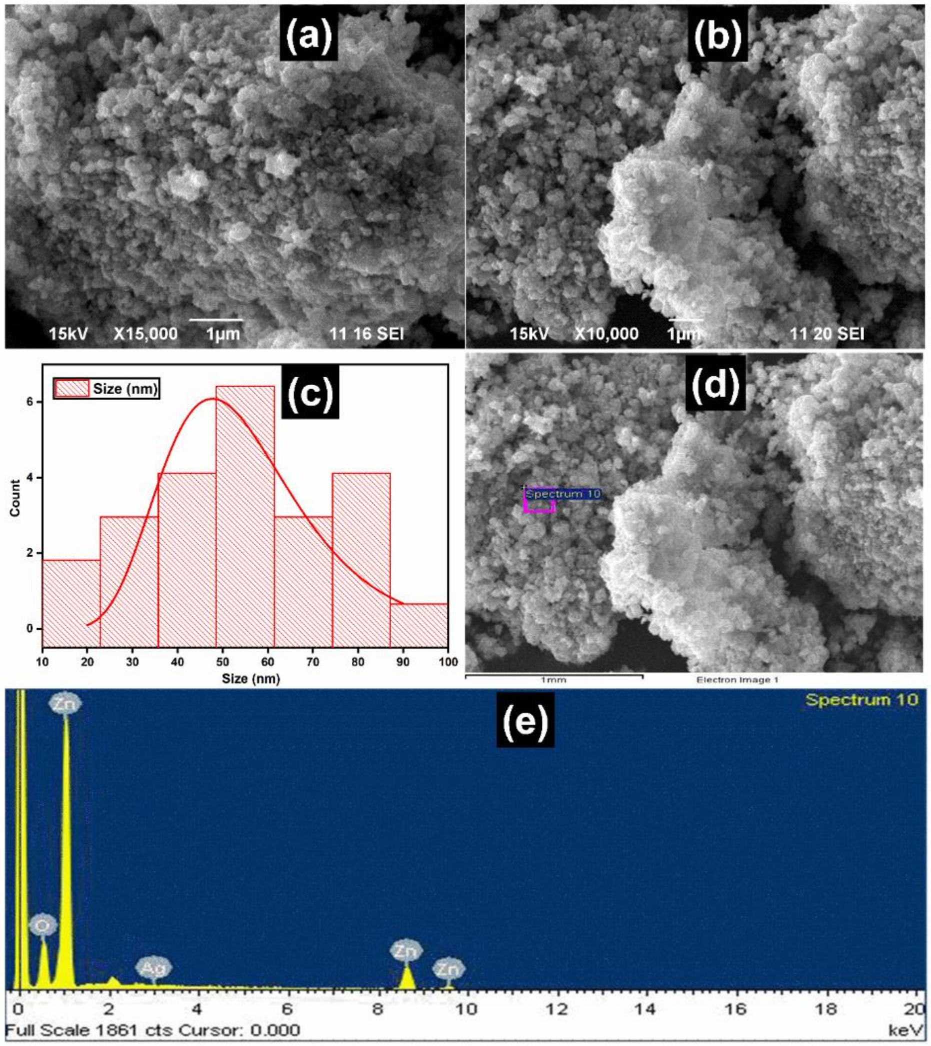

Fig. 3: (a, b, d) SEM micrographs of Ag/ZnO@MC; (c) Size distribution of particles; and (e) EDS spectrum of synthesized nanocomposite.

nanoparticles exhibited a fairly narrow size range (Fig. 3c), with the majority falling within the size range of 20–80 nm, confirming their nanoscale and uniform nature. The average diameter was 49.5 nm. The EDS spectrum displayed the characteristic signals for zinc (Zn), oxygen (O), and silver (Ag), confirming the successful incorporation of Ag onto the ZnO matrix.

XRD Analysis

The crystalline structure of Ag-doped ZnO nanoparticles was analyzed using X-ray diffraction (XRD). The diffraction pattern (Fig. 4) exhibits distinct peaks corresponding to the hexagonal wurtzite structure of ZnO (JCPDS card No. 792205). The major diffraction peaks observed at 2θ values of approximately 31.7°, 34.4°, 36.2°, 47.5°, 56.6°, 62.8°, and 67.9° are attributed to the 100, 002, 101, 102, 110, 103, and 112 planes of ZnO, respectively. There were no additional peaks corresponding other impurity phases were detected, confirming the successful incorporation of Ag ions into the ZnO lattice without altering its basic crystal structure.

The average crystallite size (D) of the Ag-doped ZnO sample was estimated using the Debye–Scherrer equation:

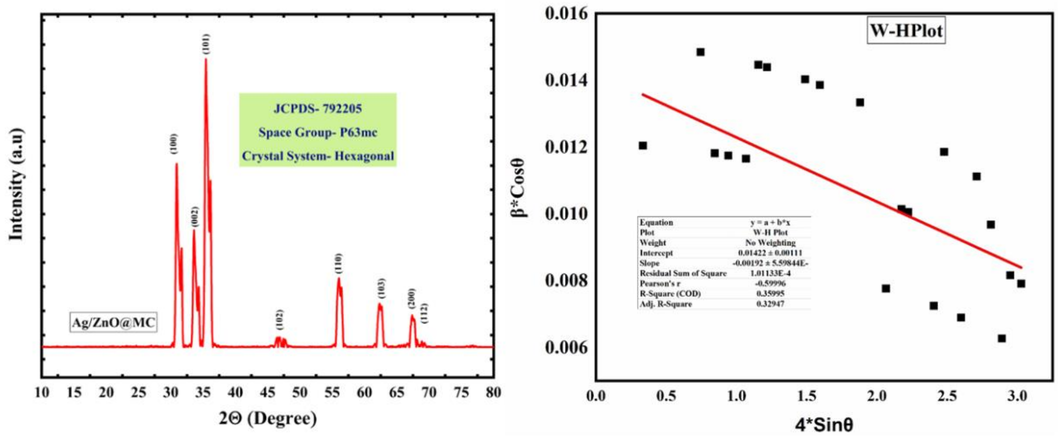

Fig. 4: (a) XRD spectrum of Ag/ZnO@MCNPs.(JCPDS No-792205); (b) Williamson–Hall (W–H) plot for Ag/ZnO nanoparticles.

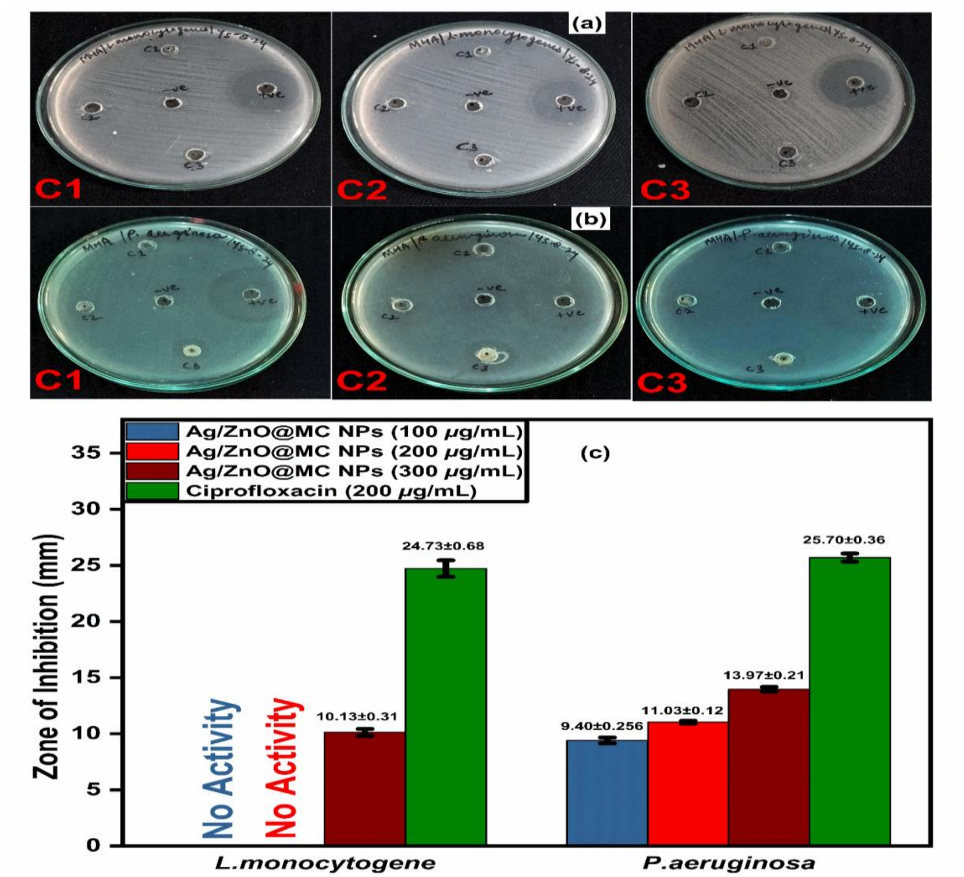

Fig. 5: (a, b) Antibacterial activity of Ag/ZnO@MC against *L. monocytogene* and *P. aeruginosa;* (c) Bar graph showing relative zone of inhibition.

$$D = \frac{K\lambda}{\beta \cos\theta}$$

Where K is the shape factor (0.9), λ is the X ray wavelength (1.5406 Å), β is the full width at half maximum (FWHM), and θ is the Bragg angle.

The calculated average crystallite size is 14.52 nm, indicating the formation of nanosized crystallites. The microstrain (ε) was calculated using the relation $\varepsilon = \beta/(4\tan\theta)$ (Fig. 4b), and its value was found to be 0.00048, suggesting minimal

Table 1: Effect of Ag/ZnO@MC NPs on chosen microbial strains

Dose Concentration (μg/ml)	Zone of Inhibition (mm); mean ±SD			
	P. aeruginosa	***L. monocytogenes***	**Positive Control**	**Negative Control**
100	9.40 ± 0.256	Nil	—	Nil
200	11.03 ± 0.12	Nil	25.70 ± 0.36 (*P. aeruginosa*) 24.73 ± 0.68 (*L. monocytogenes*)	Nil
300	13.97 ± 0.21	10.13 ± 0.31	—	Nil

Table 2: Some selected reports for comparison to synthesized Ag/ZnO@MC

S. No.	Plant extract	Material	Shape	Size (nm)	Bacterial Species	Concentration (μg/ml)	ZOI (mm)	Ref.
1	*Macrotyloma uniflorum*	Ag/ZnO	Spherical	90	*B. subtilis*	500	12±1.5	Sali *et al.* (2021)
					Streptococcus		11±0.6	
					E. coli		8±0.3	
2	*Vitis vinifera*	Ag/ZnO	Spherical	20	*E. coli*	100	9.00± 0.42	Naseer and Iqbal (2024)
					S. aureus		8.00± 0.53	
3	*Ruta chalepensis*	Ag/ZnO	-	-	*S. aureus*	5000	11 ± 1.0	Hunde Gonfa and Lealem Birhanu (2024)
					B. subtilis		12.33± 0.57	
					E. coli		11 ± 1.0	
					S. typhi		10.67± 0.57	
4	*Trigonella foenum-graecum*	Ag/ZnO	Spherical	75	*S. aureus*	2000	13.5±0.707	Noohpisheh *et al.* (2020)
					E. coli		12.5± 0.707	
5	*Acer palmatum*	Ag/TiO_2			*S. aureus*	400	7.6	Hidayat *et al.* (2024)
					E. coli		9.1	
6	*Cucumis maderaspatanus*	Al/ZnO	Hexagonal	25	*K. bacillus*	1000	2.65± 0.15	Sugitha *et al.* (2024)
					E. coli		No Activity	
					V. cholera		1.98± 0.03	
					B. subtilis		1.01± 0.01	
					S. aureus		4.01± 0.01	
					S. mutans		0.67± 0.01	
7	Madras Carpet	Ag/ZnO@MC	Spherical	49.4	*L. monocytogenes*	300	10.13± 0.31	**Present Work**

lattice distortion in the sample.

A slight shift in peak position and change in FWHM compared to standard ZnO pattern confirms the incorporation of Ag into the ZnO crystal lattice, leading to minor lattice strain due to ionic size mismatch between Ag^+ and Zn^{2+} ions (Lefatshe *et al.*, 2021). The small crystallite size and low strain value indicate good crystallinity and uniform particle distribution.

Antibacterial Activity

Biosynthesized Ag/ZnO@MC NPs has shown enhanced antibacterial activity against two distinct bacterial strains: Gram-positive (*Listeria monocytogenes*) and Gram-negative (*Pseudomonas aeruginosa*)(Fig. 5); the result is summarized in Table 1.

P. aeruginosa possesses a complex cell wall structure made up of three layers: peptidoglycan, a lipoprotein layer, and an outer lipopoly-saccharide membrane that enriches its surface with electrostatically negative charges, contributing to its defense against many antibacterial agents (MacNair and Tan, 2023). On the other hand, *L. monocytogenes*, a Gram-positive bacterium, has a simpler cell wall architecture comprising a thick peptidoglycan layer and teichoic acids but lacks an outer membrane (Renier *et al.*, 2011; Rajagopal and Walker, 2016), which makes it comparatively more susceptible to nanoparticle-induced damage. Contrary to that, the synthesized material was more effective against *P. aeruginosa*. The antibacterial mechanism of Ag-ZnO NPs involves disruption of bacterial cell membranes through electrostatic interactions, generation of reactive oxygen species (ROS), and release of Zn^{2+} and Ag^{+} ions, which collectively cause oxidative stress, protein and DNA damage, and metabolic interference in bacterial cells. Notably, the enhanced activity of bimetallic Ag-ZnO NPs compared to monometallic counterparts arises from their increased surface area, synergistic effects of silver and zinc oxide components, and improved binding affinity to bacterial membranes, leading to effective inhibition of both Gram-positive and Gram-negative bacterial growth. More importantly the synthesized Ag/ZnO@MC have shown better antibacterial activity against *P. aeruginosa* which is placed under the category of "priority pathogen" by WHO, as they possess significantly higher level of resistance to various antibiotics (Specially, carbapenem-resistant)(Sati *et al.*, 2025), high-lighting the importance of Ag/ZnO@MC. Table 2 enlists some selected studies on antibacterial investigation of metal/semiconductor nano-composites for the comparison to Ag/ZnO@MC.

The material (Ag/ZnO@MC) outperformed other materials presented in Table 2, in terms of antibacterial activity against both kinds of bacterium.

Conclusion

Plant extract of Madras Carpet (*Grangea maderaspatana*) were used to successfully synthesize Ag-doped ZnO nanoparticles, demonstrating that this approach is non-toxic, economical, and environmentally benign. UV-visible, XRD and SEM analyses of the structural properties of the synthesized Ag-doped ZnO nanostructures verified that the nanoparticles have a mixture of roughly spherical and some other randomforms, with an average diameter of 49.5 nm. XRD showed highly crystalline nature of Ag/ZnO@MC with average crystallite size of 14.52 nm. UV-visible absorption spectrum exhibited a prominent peak at 379 nm and Tauc Plot suggested the band gap of the material to be 2.21 eV. The antibacterial efficacy of the material was established against two bacterial strains *L. monocytogenes* and *P. aeruginosa*, at the maximum tested dose of 300 µg/ml, 10.13 ± 0.31 mm and 13.97 ± 0.21 mm zone of inhibition observed, respectively.

Ethical Statement

The authors claim that the work presented in this manuscript is scientifically ethical. All experimental procedures were performed in accordance with the institutional regulations and relevant laboratory safety guidelines.

Author Contributions

Shukla Yogesh Kumar and *Pandey Priyansh*: equally contributed, Performed experimental work, conducted formal analysis, and wrote the original manuscript; *Srivastava Ashok Kumar*: Data curation, validation, formal analysis, Review and Editing**;** *Pandey Janardan Prasad*: scientific and financial support; *Kumar Jitendra*: Conceptualization, critical analysis, mentoring, and data analysis of the study; and *Shukla Alok*: Supervision, validation, formal analysis and data analysis. All authors have read and agreed to the published version of the manuscript.

Acknowledgements

The authors acknowledge M.L.K.P.G. College, Balrampur for providing the necessary facilities to conduct this research successfully. We also thank the University Sophisticated Instrumentation Centre (USIC) at B.B.A.U. Lucknow, for enabling the FTIR, and SEM with EDS analyses, and CytoGene Research and Development LLP for conducting antimicrobial analyses.The authors acknowledge the financial support for this research from the Directorate of Higher Education, Government of Uttar Pradesh (UP) sanctioned vide Letter Reference No. number-81/2024/1042/ seventy-4-2024-002-4(33)/2023, dated 25 September 2024, Project number 84.

Conflict of Interest

The authors declare no conflicts of interest.

References

Aldeen TS, Ahmed Mohamed HE and Maaza M. (2022) ZnO nanoparticles prepared via a green synthesis approach: Physical properties, photocatalytic and antibacterial activity. J Physics Chem Solids 160: 110313.

Atherton K, Newbold G and Hockey J. (1971) Infra-red spectroscopic studies of zinc oxide surfaces. Discussions Faraday Soc. 52: 33-43.

Bahramikia S and Izadi R. (2023) Plant-based green synthesis of nanoparticles as an effective and safe treatment for gastric ulcer. Inflammopharmacol. 31(6): 2843-2855.

Baig A, Siddique M and Panchal S. (2025) A review of visible-light-active zinc oxide photocatalysts for environmental application. Catalysts 15(2): 100.

Deepa Rani S, Abiramy Neveda TR, Shettu N, Mahendrakumar M and Baranitharan M. (2025) Eco-friendly control of disease-transmit mosquito vectors using the mosquito fish *Gambusia affinis* and low dosages of *Mukia maderaspatana* extracts. J Chem Health Risks 15(1): 874-891.

El-Seedi HR, Omara MS, Omar AH, Elakshar MM, Shoukhba YM, Duman H, Karav S, Rashwan AK, El-Seedi AH and Altaleb HA. (2024) Updated review of metal nanoparticles fabricated by green chemistry using natural extracts: Biosynthesis, mechanisms, and applications. Bioengineering 11(11): 1095.

Hidayat R, Fadillah G, Ohira SI, Fajarwati FI, Setyorini DA and Saputra A. (2024) Facile green synthesis of Ag doped TiO_2 nanoparticles using maple leaf for bisphenol-A degradation and its antibacterial properties. Materials Today Sustainability 26: 100752.

Hunde Gonfa M and Lealem Birhanu A. (2024) Green synthesis, characterization and antibacterial evaluation of ZnO and Ag-doped ZnO nanoparticles using Ruta chalepensis leaf extract. Green Chem Letts Rev. 17(1): 2412613.

Iqbal Y, Malik AR, Iqbal T, Aziz MH, Ahmed F, Abolaban FA, Ali SM and Ullah H. (2021) Green synthesis of ZnO and Ag-doped ZnO nanoparticles using Azadirachta indica leaves: Characterization and their potential antibacterial, antidiabetic, and wound-healing activities. Materials Letters 305: 130671.

Jose' Luis CH, Sczancoski JC, Euclydes M J and Pinto AH. (2022) Methods for the synthesis of ceramic materials with perovskite structure. In: Perovskite Ceramics: Recent Advances and Emerging Applications, (eds.) Jose' Luis C.H. and Victor Anthony G.R., Elsevier, pp. 31-76.

Kandav G and Sharma T. (2024) Green synthesis: an eco friendly approach for metallic nanoparticles synthesis. Particulate Sci Technol. 42(5): 874-894.

Kirubakaran D, Wahid JBA, Karmegam N, Jeevika R, Sellapillai L, Rajkumar M and Senthil Kumar K. (2025) A comprehensive review on the green synthesis of nanoparticles: advancements in biomedical and environmental applications. Biomed Materials Devices 4: 388-413.

Lefatshe K, Muiva C and Madhuku M. (2021) Effect of low energy Ag^+ ION implantation ON ZnO nanorods for enhanced visible light absorption-structural and optical analysis. Optical Materials 122: 111757.

Liu H, Feng J and Jie W. (2017) A review of noble metal (Pd, Ag, Pt, Au)–zinc oxide nanocomposites: synthesis, structures and applications. J Materials Sci Materials Electronics 28(22): 16585-16597.

MacNair CR and Tan MW. (2023) The role of bacterial membrane vesicles in antibiotic resistance. Annals New York Acad Sci. 1519(1): 63-73.

Naseer H and Iqbal T. (2024) Green synthesis of silver-doped zinc oxide nanoparticles for investigation of their photocatalytic activity and shelf life applications. Biomass Conversion Biorefinery 14(18): 21895-21911.

Noohpisheh Z, Amiri H, Farhadi S and Mohammadi-gholami A. (2020) Green synthesis of Ag-ZnO nanocomposites using *Trigonella foenum-graecum* leaf extract and their antibacterial, antifungal, antioxidant and photocatalytic properties.

Spectrochimica Acta Part A Molec Biomolec Spectrosc. 240: 118595.

Pandey P, Shukla YK, Pandey JP, Singh PK and Kumar J. (2025) Plant-mediated synthesis of ZnO nanomaterials using pumpkin flower (*Cucurbita pepo*) extract and its antibacterial and photocatalytic properties. Biomass Conversion Biorefinery 15(11): 17565-17576.

Rajagopal M and Walker S. (2017) Envelope structures of gram-positive bacteria. Curr Top Microbiol Immunol. 404: 1-44.

Rathika A and Irine T. (2022) Synthesis of silver (Ag) doped zinc oxide (ZnO) nanoparticles as efficient photocatalytic activity for degradation methylene blue dye. J Adv Sci Res. 13(2): 129-135.

Renier S, Hébraud M and Desvaux M. (2011) Molecular biology of surface colonization by *Listeria monocytogenes*: an additional facet of an opportunistic Gram-positive foodborne pathogen. Environ Microbiol. 13(4): 835-850.

Sali RK, Pujar MS, Patil S and Sidarai AH. (2021) Green synthesis of ZnO and Ag-ZnO nanoparticles using macrotyloma uniflorum: evaluation of antibacterial activity. Adv Materials Letts. 12(7): 1-7.

Saravanadevi K, Kavitha M, Karpagavinayagam P, Saminathan K and Vedhi C. (2022) Biosynthesis of ZnO and Ag doped ZnO nanoparticles from *Vitis vinifera* leaf for antibacterial, photocatalytic application. Materials Today Proc. 48: 352-356.

Sati H, Carrara E, Savoldi A, Hansen P, Garlasco J, Campagnaro E, Boccia S, Castillo-Polo JA, Magrini E, Garcia-Vello P, Wool E, Gigante V, Duffy E, Cassini A, Huttner B, Pardo PR, Naghavi M, Mirzayev F, Zignol M, Cameron A, Tacconelli E; and WHO Bacterial Priority Pathogens List Advisory Group (2025) The WHO Bacterial Priority Pathogens List 2024: a prioritisation study to guide research, development, and public health strategies against antimicrobial resistance. Lancet Infect Dis. 25(9): 1033-1043.

Shreema K, Mathammal R, Kalaiselvi V, Vijayakumar S, Selvakumar K and Senthil K. (2021) Green synthesis of silver doped zinc oxide nanoparticles using fresh leaf extract Morinda citrifoliaand its antioxidant potential. Materials Today Proc. 47: 2126-2131.

Shukla YK, Pandey P, Pandey JP, Shukla A and Kumar J. (2025) Duckweed extract-mediated green synthesis of ZnO nanoparticles and its antibacterial, antioxidant, and photocatalytic properties. Biomass Conversion Biorefinery 15(14): 21477-21491.

Sugitha SKJ, Latha RG, Venkatesan R, Kim SC, Vetcher AA and Khan MR. (2024) Green synthesis of Al-ZnO nanoparticles using *Cucumis maderaspatanus* plant extracts: Analysis of structural, antioxidant, and antibacterial activities. Nanomaterials 14(22): 1851.

Thanuja G, Mishra S and Kumar S. (2024) *Grangea maderaspatana* (L.) Poir.: A medicinal herb of India. In: Medicinal Asteraceae of India, (eds.) Gucchait K.C., Lal S., Kumar S. and Mishra S., Volume I, APRF Publishers, pp. 25-32.

Triphati A and Pirzadah TB. (2023) Synthesis methods of nanoparticles and their key applications. In: Synthesis of bionanomaterials for biomedical applications, (eds.) Ozturk M., Roy A., Bhat R.A., Vardar-sukan F. and Tonelli Fernanda M.P., Elsevier, pp. 57-76.

Verma R, Chauhan A, Shandilya M, Li X, Kumar R and Kulshrestha S. (2020) Antimicrobial potential of Ag-doped ZnO nanostructure synthesized by the green method using *Moringa oleifera* extract. J Environ Chem Engineer. 8(3): 103730.